

STMARL: A Spatio-Temporal Multi-Agent Reinforcement Learning Approach for Traffic Light Control

Yanan Wang

School of Computer Science and
Technology, University of Science and
Technology of China
ynwang@mail.ustc.edu.cn

Tong Xu

School of Computer Science and
Technology, University of Science and
Technology of China
tongxu@ustc.edu.cn

Xin Niu

iFLYTEK Research
xinniu2@iflytek.com

Chang Tan

iFLYTEK Research
changtan2@iflytek.com

Enhong Chen

School of Computer Science and
Technology, University of Science and
Technology of China
cheneh@ustc.edu.cn

Hui Xiong

School of Computer Science and
Technology, University of Science and
Technology of China
xionghui@gmail.com

ABSTRACT

The development of intelligent traffic light control systems is essential for smart transportation management. While some efforts have been made to optimize the use of individual traffic lights in an isolated way, related studies have largely ignored the fact that the use of multi-intersection traffic lights is spatially influenced and there is a temporal dependency of historical traffic status for current traffic light control. To that end, in this paper, we propose a novel Spatio-Temporal Multi-Agent Reinforcement Learning (STMARL) framework for effectively capturing the spatio-temporal dependency of multiple related traffic lights and control these traffic lights in a coordinating way. Specifically, we first construct the traffic light adjacency graph based on the spatial structure among traffic lights. Then, historical traffic records will be integrated with current traffic status via Recurrent Neural Network structure. Moreover, based on the temporally-dependent traffic information, we design a Graph Neural Network based model to represent relationships among multiple traffic lights, and the decision for each traffic light will be made in a distributed way by the deep Q-learning method. Finally, the experimental results on both synthetic and real-world data have demonstrated the effectiveness of our STMARL framework, which also provides an insightful understanding of the influence mechanism among multi-intersection traffic lights.

KEYWORDS

Traffic light control, multi-agent reinforcement learning, graph neural network

1 INTRODUCTION

Recent years have witnessed the increasing serious traffic congestion in most cities, which results in several negative effects like air pollution and economic losses. For instance, traffic congestion has caused the financial cost as \$305 billion in 2017 in the US, \$10 billion more than 2016 [7]. Along this line, optimal control of traffic lights has been widely used for reducing congestion. Traditionally, control plan of traffic lights was pre-defined as fixed based on historical traffic data [25, 40], or artificially regulated by officers based on current traffic status [9]. However, these solutions might be rigid and shortsighted, or even lead to the heavy burden of manpower. Thus, a more intelligent plan is still urgently required.

Thanks to the development of data analytic techniques, nowadays, traffic light control has been supported by advanced methods like *reinforcement learning* [24, 38], which effectively model the traffic status to make sequential decisions. However, though prior arts performed well, most of them are limited to the isolated intersections without coordination. Indeed, in real-world situation, control of traffic light will definitely impact the traffic status, and then results in a chain reaction on adjacent intersections. Obviously, mutual influence among multiple intersections should not be ignored during the modeling. To that end, solutions based on *multi-agent reinforcement learning* have been designed [6, 21], which further improved the performance. However, they may still face some challenges. First, the dimensionality of action space grows exponentially with the increasing number of agents, which causes dramatic complexity. Second, though distributed models may alleviate the problem of dimension explosion, it is still difficult to formulate the coordination among multiple traffic lights.

Intuitively, when describing the correlation among multiple intersections, we realize that they could be approximately formulated as *graph* structure based on spatial adjacency on the road network. Similar with information flow in graph, traffic volume in the current intersection can be naturally split for adjacent intersections, which results in the **spatial influence** among multiple traffic lights. Moreover, short periods are spent on traffic flow when moving to adjacent intersections, which further results in the **temporal dependency** among multiple traffic lights. Therefore, our challenge

Permission to make digital or hard copies of all or part of this work for personal or classroom use is granted without fee provided that copies are not made or distributed for profit or commercial advantage and that copies bear this notice and the full citation on the first page. Copyrights for components of this work owned by others than the author(s) must be honored. Abstracting with credit is permitted. To copy otherwise, or republish, to post on servers or to redistribute to lists, requires prior specific permission and/or a fee. Request permissions from permissions@acm.org.
Conference'17, July 2017, Washington, DC, USA

© 2018 Copyright held by the owner/author(s). Publication rights licensed to ACM.
ACM ISBN 978-1-4503-9999-9/18/06...\$15.00
<https://doi.org/10.1145/1122445.1122456>

has been transferred as modeling the spatio-temporal influence among multiple intersections for intelligent traffic light control.

To that end, in this work, we propose a Spatio-Temporal Multi-agent Reinforcement Learning (STMARL) framework for multi-intersection traffic light control. Specifically, we first construct the traffic light adjacency graph based on the spatial structure among traffic lights. Then, historical traffic records will be incorporated with current traffic status via Recurrent Neural Network structure. Afterwards, based on the traffic information with temporal dependency, we design a Graph Neural Network based module to represent relations among multiple traffic lights, which allows the efficient relation reasoning among the traffic lights. Finally, the distributed decision for each traffic light will be made by deep Q-learning method. Both quantitative and qualitative experiment results have demonstrated the effectiveness of our STMARL framework, which provides an insightful understanding of influence mechanism among multi-intersection traffic lights. The technical contribution of this paper could be summarized as follows:

- To the best of our knowledge, we are among the first ones who study the spatio-temporal dependency among multiple intersections, with leveraging graph structure for better modeling coordination between intersections.
- A novel multi-agent reinforcement learning framework is proposed, in which graph neural network with attention mechanism for iterative relational reasoning and the recurrent neural network is incorporated to model the spatio-temporal dependency.
- Experiments on both synthetic and real-world datasets validated the effectiveness of our solution compared with several state-of-the-art methods, and further revealed some coordination mechanism among traffic light agents.

2 RELATED WORKS

In this section, we briefly review the related works in traffic light control, methodologies of multi-agent reinforcement learning and graph neural networks.

Traffic Light Control. In the literature, traffic light control methods can be mainly divided into three types: predefined fixed-time control [25], actuated control [9] and adaptive traffic control [1, 11, 18, 24]. The predefined fixed-time control is determined offline using historical traffic data and actuated control is based on current traffic state using predefined rules. The main drawback of these two methods is that they do not take into account the long term traffic situation. Therefore, researchers began exploring adaptive traffic light control methods. Following this line, reinforcement learning methods have been used for traffic light control [2, 10, 21, 31, 38] so that the control strategy can be adaptively generated based on the current traffic state. Although reinforcement learning methods have achieved success for traffic light control in one intersection, it's still challenging for multi-intersection traffic light control task: the curse of dimensionality in the centralized model and coordination problem in a distributed model. Kuyer et al. [21] formulated the explicit coordination among agents using max-plus algorithm which estimates the optimal joint action by sending locally optimized messages among connected agents. However, this method is model-based which requires the knowledge of the environment. Besides,

the max-plus algorithm can increase control overhead and computational cost among neighboring agents significantly [39]. El-Tantawy et al. [11] proposed a approach called MARLIN-ATSC, which deals with the dimensionality problem by utilizing the principle of locality of interaction [27] and modular Q-learning technique [28]. However, the previous methods mainly ignore the spatial structure information among the traffic lights in the real world for better coordination. What's more, there is no interpretation of the coordination mechanism among these agents.

Multi-agent Reinforcement Learning. In the setting of multi-agent reinforcement learning [6, 12, 14, 29, 32], agents are optimized to learn cooperative or competitive goal. Independent DQN [33] extends DQN to multi-agent settings where each agent learns its own policy independently. Although there is a non-stationary problem for independent DQN, it often works well in practice [33, 42]. To address the issue of reinforcement learning method for multi-agent settings, Lowe et al. [23] proposed multi-agent actor-critic for mixed cooperative-competitive environments. They adopt the framework for centralized training with decentralized execution for cooperation.

Note that previous works [17, 32] mainly design heuristic rules to decide who or how many agents the target agent communicates to, while in this paper, we learn to communicate via the existing spatial structure among agents as well as temporal dependency for multi-intersection traffic light control.

Graph Neural Networks. Our proposed method is also related to recent advances of Graph Neural Network (GNN) [3, 4, 22, 30]. GNN has been proposed to learn the structured relationship, which allows for iterative relational reasoning through messaging passing [13] on the graph. Battaglia et al. [4] introduced a general framework of *Graph Networks* which unified various proposed graph network architectures to support relational reasoning and combinatorial generalization. Recently, there are some works trying to explore relational inductive biases in deep reinforcement learning. Wang et al. [37] proposed NerveNet for robot locomotion, where it modeled the bodies of robots as discrete graph structure and output action for this single agent. Zambaldi et al. [41] proposed to use relational inductive biases in deep reinforcement learning agent for StarCraft II game. However, there is no explicit graph construction which is learned from the raw visual input. Comparatively, in this paper, we explicitly construct the traffic light adjacency graph for modeling the geographical structure information to facilitate the coordination among multi-intersection traffic light control.

3 PROBLEM STATEMENT

In this section, we will first introduce the construction of *traffic light adjacency graph*, and then formally define our problem.

We first attempt to describe the road network structure in the graph perspective. In a real-world scenario, the structure of the intersections could be complicated. For instance, as shown in Figure 1 (a), those roads, which are connected to the same intersection, may hold a different amount of lanes (1-5) and different directional constraint (two-way or one way). To describe the complicated settings, we construct the *traffic light adjacency graph* as $G = (V, E)$, as shown in Figure 1 (b). Specifically, V denotes the nodes, including the *control nodes* which contain the traffic lights (blue nodes), and

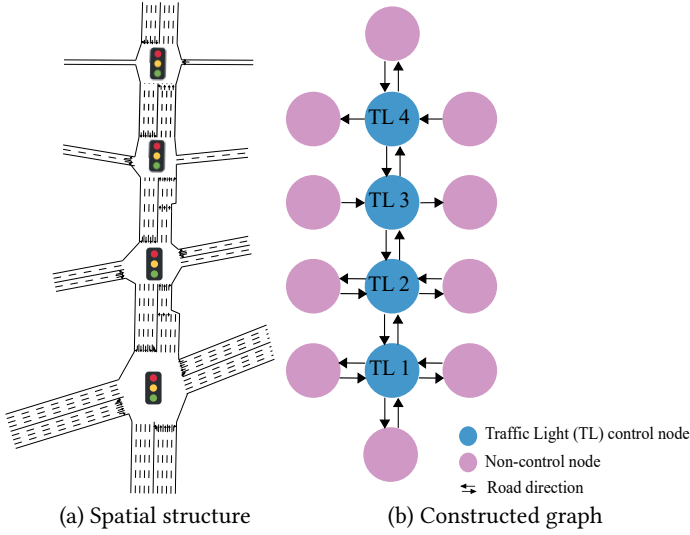


Figure 1: An illustration of the traffic light adjacency graph structure in the real world.

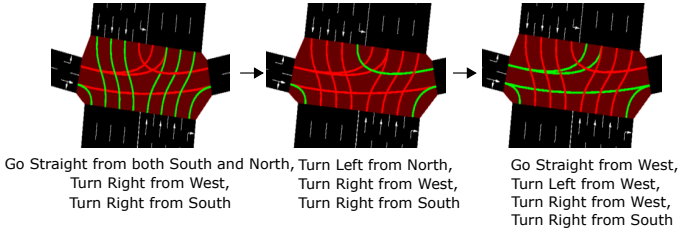


Figure 2: One sample of fixed phase order in a cycle used in the real world with the meaning of each traffic light phase.

non-control nodes which indicate the endpoints (pink nodes). At the same time, E denotes the edges, in which e_k indicates the directed road to connect two nodes with the type $c(k)$, meaning the number of lanes l_k in this directed road. Definitely, we use a unidirectional edge in G to present each one-way road, and each two-way road is presented by two edges with opposite directions.

Based on the constructed *traffic light adjacency graph*, we then turn to study the problem of multi-intersection traffic light control in the view of *multi-agent reinforcement learning*. Specifically, we treat each traffic light as one *agent*, and the group of traffic light agents is learned cooperatively to maximize the global reward (e.g., minimize the overall queue length in this area). Along this line, the multi-intersection traffic light control problem could be defined as a *Markov Decision Process* (MDP) for N agents within finite steps. Moreover, considering that the recorded information might be incomplete and inaccurate, we further extend the MDP problem as *Partially-Observable Markov Decision Process* (POMDP), which can be defined as a tuple $(N, S, O, \mathcal{A}, \mathcal{P}, \mathcal{U}, \mathcal{R}, \gamma)$, in which N denotes the number of agents, and the rest are listed as follows:

- **State Space** \mathcal{S} : $s_{i,t} \in \mathcal{S}$ is the fully observable system state, which consists of all the information in the traffic light adjacency

Table 1: Mathematical Notations

Notation	Description
$o_{i,t}$	Observation for agent i at time t
$a_{i,t}$	Action for agent i at time t
$r_{i,t}$	Reward for agent i at time t
$Q_{i,t}$	Q value for agent i at time t
q_l	Queue length in the lane l
n_l	Number of vehicles in the lane l
w_l	Updated waiting time for all vehicles on the lane l
l_k	Lanes number in the k -th edge
$c(k)$	Edge type for the k -th edge
ϵ	Exploration probability
\mathcal{D}	Memory buffer
G	$G = (V, E)$ is the constructed traffic light adjacency graph
G_t^{in}	Traffic light graph (node $v_{i,t}^{in}$) after edge update at time t
G_t^{hid}	Output hidden state (node $v_{i,t}^{hid}$) of graph LSTM at time t
G_t^{out}	Traffic light graph (node $v_{i,t}^{out}$) after node update at time t
$v_{i,t}^d$	Node i 's vector after relation reason step d at time t
$f_e^{c_k}$	Edge encoder for edge type of c_k
Δ_t	Time interval to consider the temporal dependency

graph at time t for agent i . Usually, this true state is not directly accessible by the each traffic light agent. Besides, the agent can only have local view, which causes the partial observability problem.

- **Observation Space** \mathcal{O} : $o_{i,t} \in \mathcal{O}$ is the partially observable state for agent i at time t . In the graph G , the traffic information is observed on each edge: $e_k = \{\{q_l\}_{l=1}^{l_k}, \{n_l\}_{l=1}^{l_k}, \{w_l\}_{l=1}^{l_k}\}$, where q_l, n_l, w_l are the queue length, number of vehicles and updated waiting time of vehicles in lane l respectively. Note that the partially observed state for agent i is defined as the edges information whose receiver node is node i . It is also straightforward to incorporate other complex features into the observation representation, while we focus on designing a novel framework for multi-intersection traffic light control in this paper.
- **Action** \mathcal{A} : $a_t = \{a_{i,t}\}_{i=1}^N \in \mathcal{A}$ is the joint action for all the traffic light agents at time t . In this problem, the traffic light phases for each intersection only change in a fixed phase order as shown in Figure 2 due to the constraints and safety issues in the real-world setting. Therefore, for each agent i , $a_{i,t} \in \{0, 1\}$ indicating switch to the next phase (1) or keep current phase (0), which is also commonly used in previous works [5, 24, 38].
- **Reward** \mathcal{R} : $r_{i,t}$ is the immediate reward for agent i at time t . Traffic agent i is optimized to maximize the expected future return $\mathbb{E}[\sum_{t=1}^T \gamma^{t-1} r_{i,t}]$, where γ is the discount factor. The individual reward $r_{i,t}$ for agent i is $r_{i,t} = -\sum_{l=1}^{l_i} q_l$, where l_i is the number of incoming lanes connected to intersection i .
- **State Transition Probability** \mathcal{P} : $p(s_{t+1}|s_t, a_t)$ defines the probability of transition from state s_t to s_{t+1} when all the agents take joint action a_t .
- **Observation Probability** \mathcal{U} : This is the probability of observation $o_{t+1}, o_{t+1} \sim \mathcal{U}(o_{t+1}|s_{t+1}, a_t)$.

Based on the formulations above, we can formally define the problem of multi-intersection traffic light control as follows, and related mathematical notations are summarized in Table 1.

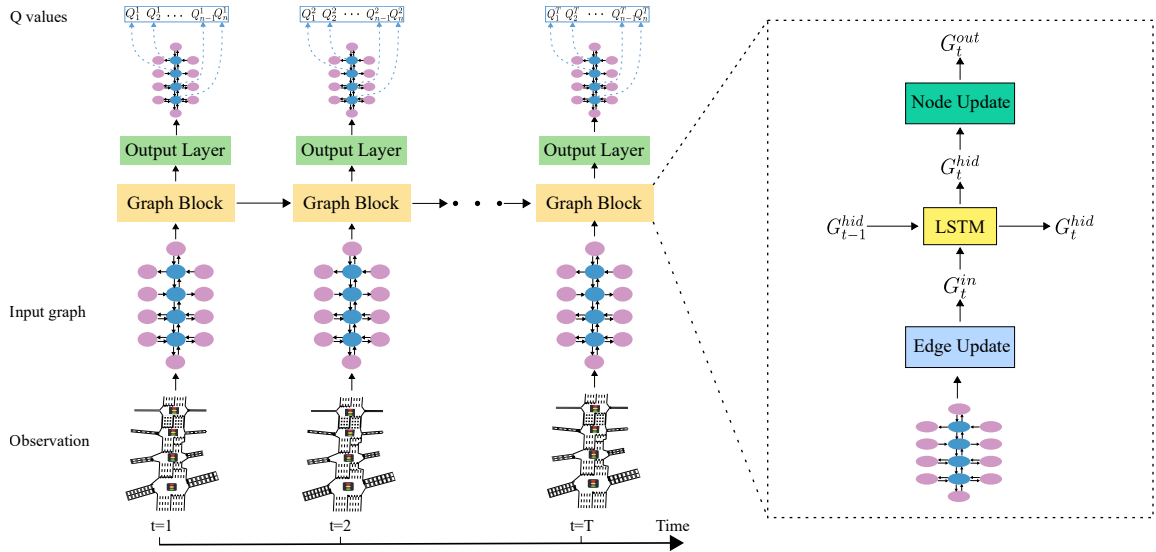


Figure 3: Overall Q-network for Spatio-Temporal Multi-Agent Reinforcement Learning.

Definition 3.1. (Problem Definition). Given the traffic light adjacency graph G , as well as the potential reward $r_{i,t}$ for each action $a_{i,t}$ made by every traffic light agent i at time t , we target at making proper decisions $a_{i,t}$ for each traffic light agent i , so that the global reward $\sum_{i=1}^N r_{i,t}$ will be maximized.

4 SPATIO-TEMPORAL MULTI-AGENT REINFORCEMENT LEARNING

In this section, we will introduce our Spatio-Temporal Multi-Agent Reinforcement Learning (STMARL) framework in detail for multi-intersection traffic light control.

4.1 Overview

The overall framework of STMARL is illustrated in Figure 3. To be specific, we construct the graph consisting of the traffic light agents, and then use the graph block to learn *spatial structure information* on the input graph, with considering the historical traffic state as incorporating *temporal dependency*.

The module inside the graph block is shown in the right part of Figure 3, which includes:

- An *edge update* module, to update the edge information;
- A *recurrent neural network* variant, namely Long Short Term Memory unit (LSTM) [16] to summarize historical traffic information in hidden state to learn *temporal dependency*;
- A *node update* module, to update state of each traffic light.

Along this line, each agent has interactions with other traffic light agents, which is beneficial for the multi-intersection traffic light control in a system level. At the same time, the problem of partial observability will be handled. In the following subsections, we will introduce all these modules in detail.

4.2 Base Multi-agent Reinforcement Learning

Firstly, we will briefly introduce the base multi-agent reinforcement learning method which is based on the Independent DQN [34], where each agent i learns the independent optimal function Q_i separately without cooperation. Formally, for each agent i , we have the observation $o_i = \{q_l, n_l, w_l\}_{l=1}^{l_i}$, where l_i is the number of incoming lanes which are connected to intersection i . We target at minimizing the following loss:

$$\mathcal{L}_i(\theta_i) = \mathbb{E}_{(o_{i,t}, a_{i,t}, r_{i,t}, o_{i,t+1}) \sim \mathcal{D}} \left[(y_{i,t} - Q(o_{i,t}, a_{i,t}; \theta_i))^2 \right], \quad (1)$$

$$y_{i,t} = r_{i,t} + \gamma \max_{a'} Q(o_{i,t+1}, a'; \theta_i^{tar}), \quad (2)$$

where θ_i^{tar} is the target Q-network updated periodically to stabilize training. Also, \mathcal{D} is the replay buffer to store the state transitions.

For the Independent DQN, to reduce the parameters of the Q-network which scale with the number of traffic light agents, it's reasonable to share the parameters of Q-network among agents.

4.3 Learning Spatial Structure Dependency

Then, we turn to introduce the learning process inside graph block, which considers the *spatial structure information* between the traffic light agents for better coordination. Generally, traffic light agents in the base model only learn their own policy independently without explicit coordination, and observation state $o_{i,t}$ in the base model simply concatenates the traffic information in incoming lanes connected to intersection i , which ignores the spatial structure information. Therefore, a more comprehensive framework is required to leverage the spatial structure of these traffic lights for better coordination, so that the global traffic situation will be optimized.

4.3.1 Edge Update. As the traffic information is observed in the graph edges as stated in Section 3, we firstly introduce the edge update module. In this problem, the traffic information is first collected by each edge e_k , where $e_k = \{\{q_l\}_{l=1}^{l_k}, \{n_l\}_{l=1}^{l_k}, \{w_l\}_{l=1}^{l_k}\}$ and

$e_k \in \mathbb{R}^{l_k \times 3}$. To transform the raw input into embedded observation vector, edge encoder for different edge types is applied per edge to encode the collected message. Edge e_k is updated as follows:

$$e'_k = f_e^{c(k)}(e_k). \quad (3)$$

To reduce parameters of edge encoder $f_e^{c(k)}$ for different edge types, separate parameters are used for the first layer of edge encoder to encode the input with different dimensions, but parameters for the other layers are shared. Specifically, we use two-layer MultiLayer Perceptron (MLP) with ELU [8] activation function.

After updating the edge information, nodes' representations are obtained by aggregating each node's receiver edges. Here we denote the graph with initial node values as G_t^{in} with nodes $V = \{v_{i,t}^{in}\}_{i=1}^N$, where initial representation $v_{i,t}^{in}$ at time t is obtained as follows:

$$v_{i,t}^{in} = \sum_{k, rec_k=i} e'_k, \quad (4)$$

where rec_k is the receiver node of the k -th edge.

4.3.2 Node Update. Then, we turn to introduce the node update module to model the interaction relationship among these agents. Here, we use attention mechanism [35, 36] to leverage the spatial structure information and perform relation reasoning among these agents. Specifically, at relation reasoning step d , the input node vector consists of both the initial node vector $v_{i,t}^{in}$ and the node vector $v_{i,t}^{d-1}$ in previous relation reasoning step $d-1$:

$$\hat{v}_i = [v_{i,t}^{in} \| v_{i,t}^{d-1}], \quad (5)$$

where $\|$ represents the concatenation operation.

Then, we compute the attention score α_{ij} between node i and its sending nodes $j \in \mathcal{N}_i$ where the edge direction is from j to i :

$$\alpha_{ij} = \frac{\exp\left(f\left(a^T [\hat{v}_i \| \hat{v}_j]\right)\right)}{\sum_{k \in \mathcal{N}_i} \exp\left(f\left(a^T [\hat{v}_i \| \hat{v}_k]\right)\right)}, \quad (6)$$

where a is the trainable weight vector and f is the nonlinear activation function and here we use ELU function. Then the aggregated attention information \bar{v}_i from the sending nodes for node i is:

$$\bar{v}_i = \sum_{j \in \mathcal{N}_i} \alpha_{ij} \hat{v}_j. \quad (7)$$

Finally, the node vector $v_{i,t}^d$ is updated based on its own information and the aggregated neighbor information:

$$v_{i,t}^d = g([\hat{v}_i \| \bar{v}_i]), \quad (8)$$

where g is one-layer MLP with ELU activation in the MLP output layer.

The above node update process is for one step relation reasoning. Multi-step relation reasoning can be performed to capture the high-order interaction among the agents. The output graph at time t is denoted as G_t^{out} with nodes $V = \{v_{i,t}^d\}_{i=1}^N$.

4.4 Learning Temporal Dependency

Moreover, we attempt to learn *temporal dependency* to incorporate the historical traffic state. As the traffic state is highly dynamic over the time, to model the temporal dependency and handle the partial observability in the POMDP problem, we use the recurrent

Algorithm 1 Spatio-Temporal Multi-Agent Training

Require: Traffic light adjacency graph $G = (V, E)$.

- 1: Initialize the parameters of Q-network and target Q-network with pretrained weights.
 - 2: **for** epoch = 1 to max-epochs **do**
 - 3: Reset the environment.
 - 4: **for** $t = 0$ to T **do**
 - 5: Get observation o_t of the traffic light adjacency graph state.
 - 6: **for** agent $i = 1$ to N **do**
 - 7: Compute $v_{i,t}^{hid}$ using Eq(9). \triangleright learning temporal dependency
 - 8: Compute node update result $v_{i,t}^{out}$ using Eq(8). \triangleright learning spatial structure dependency
 - 9: Compute Q values $Q_{i,t}$ using Eq(11).
 - 10: With probability ϵ pick random action $a_{i,t}$, else $a_{i,t} = \max_{a'} Q_{i,t}(a')$.
 - 11: **end for**
 - 12: Execute joint action $a_t = \{a_{i,t}\}_{i=1}^N$ in the environment and get reward $r_t = \{r_{i,t}\}_{i=1}^N$ and next observation o_{t+1} .
 - 13: Store transition (o_t, a_t, o_{t+1}, r_t) into \mathcal{D} .
 - 14: **end for**
 - 15: **for** $c = 1$ to $C1$ **do**
 - 16: Sample a random batch of transitions over continues time interval $\Delta_t: \{o_t, a_t, r_t, o_{t+1}\}_{t=1}^{\Delta_t}$ from \mathcal{D} .
 - 17: For each agent i at time t compute target:

$$y_{i,t} = r_{i,t} + \gamma \max_{a'} Q_{i,t+1}(a'; \theta^{tar}).$$
 - 18: Update Q-network:

$$\theta \leftarrow \theta - \nabla_{\theta} \sum_{i=1}^N \sum_{t=1}^{\Delta_t} (y_{i,t} - Q_{i,t}(a_{i,t}; \theta))^2.$$
 - 19: **end for**
 - 20: **end for**
-

neural network to incorporate the historical traffic information. Specifically, we process the nodes in current input traffic state graph G_t^{in} and the last time hidden graph G_{t-1}^{hid} using LSTM. The output hidden graph G_t^{hid} with nodes $V = \{v_{i,t}^{hid}\}_{i=1}^N$ is:

$$\begin{aligned} i_t &= \sigma\left(W_i \left[v_{i,t}^{in}, v_{i,t-1}^{hid}\right] + b_i\right), \\ f_t &= \sigma\left(W_f \left[v_{i,t}^{in}, v_{i,t-1}^{hid}\right] + b_f\right), \\ \tilde{C}_t &= \tanh\left(W_C \left[v_{i,t}^{in}, v_{i,t-1}^{hid}\right] + b_C\right), \\ C_t &= f_t \odot C_{t-1} + i_t \odot \tilde{C}_t, \\ o_t &= \sigma\left(W_o \left[v_{i,t}^{in}, v_{i,t-1}^{hid}\right] + b_o\right), \\ v_{i,t}^{hid} &= o_t \odot \tanh(C_t), \end{aligned}$$

where, $W_f, W_i, W_C, W_o, b_f, b_i, b_C, b_o$ are parameters of weight matrices and biases. \odot represents element-wise multiplication and σ is the sigmoid function. The above process is denoted in short as:

$$v_{i,t}^{hid} = LSTM(v_{i,t}^{in}, v_{i,t-1}^{hid}). \quad (9)$$

After getting the gated hidden graph G_t^{hid} at time step t , *Node update* process in 4.3.2 is performed on the updated traffic input graph G_t^{hid} as is shown in the right part of Figure 3.

Table 2: Statistics of the real-world traffic dataset.

Time Range	Arrival Rate (cars/s)			
	Mean	Std	Min	Max
11/06/2018-11/12/2018	0.061	0.071	0.003	0.234

4.5 Output Layer

Finally, the distributed decision for each traffic light agent is now available with the learned representations for traffic lights. Based on the above learned *spatial-temporal dependency* representation, at each time t , we output the decision of whether to switch to the next traffic light phase. As there are two kinds of nodes: traffic light control nodes and non-control nodes shown in Figure 1, we process for the traffic light control nodes. For these traffic light agents, we use residual connection which concatenate the initial node vector $v_{i,t}^{in}$ and the updated node vector $v_{i,t}^{out}$:

$$x_{i,t} = [v_{i,t}^{in} \| v_{i,t}^{out}]. \quad (10)$$

Then, Q value for each agent i at time t is computed as follows:

$$Q_{i,t} = \phi(x_{i,t}), \quad (11)$$

where ϕ is two layer MLP with RELU activation, $Q_{i,t} \in \mathbb{R}^{|\mathcal{A}|}$ and we denote $Q_{i,t}(a)$ as the Q value for action a .

4.6 Training

Besides, we briefly introduce the technical solution of training process. During training, we store the observations into the replay buffer \mathcal{D} for experience replay [26]. As the observations are in the edges of graph G , we denote the observation at time t as $o_t = \{e_{k,t}\}_{k=1}^{|E|}$. We store the transition (o_t, a_t, o_{t+1}, r_t) into \mathcal{D} , where joint action $a_t = \{a_{i,t}\}_{i=1}^N$ and reward for each agent $r_t = \{r_{i,t}\}_{i=1}^N$. The training loss of Q-network for STMARL model is:

$$\mathcal{L}(\theta) = \mathbb{E}_{\{o_t, a_t, r_t, o_{t+1}\}_{t=1}^{\Delta t} \sim \mathcal{D}} \sum_{i=1}^N \sum_{t=1}^{\Delta t} (y_{i,t} - Q_{i,t}(a_{i,t}; \theta))^2, \quad (12)$$

$$y_{i,t} = r_{i,t} + \gamma \max_{a'} Q_{i,t+1}(a'; \theta^{tar}), \quad (13)$$

where Δt is the time interval. We use recurrent neural network over the continuous time interval Δt to learn temporal dependency as stated in 4.4. The influence of the temporal dependency interval is illustrated in experiment part. To stabilize training, we update the model at the end of each episode. Detailed training algorithm for Spatio-Temporal Multi-Agent Training is listed in Algorithm 1.

5 EXPERIMENTS

In this section, we conduct both quantitative and qualitative experiments to validate the effectiveness of the proposed STMARL model for multi-intersection traffic light control.

5.1 Experimental Setup

5.1.1 Synthetic Dataset. In the experiment, synthetic data is generated to test our model under different scale of road networks and various traffic patterns. The details are introduced as follows:

Table 3: Traffic light phase configurations in different time for different traffic lights in the real-world dataset.

Traffic Light Id	Time Range	Phase ID (In Order)
Traffic Light 1	0:00-6:00	12, 13, 14, 15, 16
	6:00-20:30	12, 13, 14, 15, 16
	20:30-24:00	12, 13, 14, 15, 16
Traffic Light 2	0:00-24:00	8, 9, 10, 11
Traffic Light 3	0:00-6:30	4, 5
	6:30-20:30	6, 7, 5
	20:30-24:00	4, 5
Traffic Light 4	0:00-6:30	0, 1
	6:30-20:30	2, 3, 1
	20:30-24:00	0, 1

Table 4: Selected time range of one episode for simulation for the real-world dataset.

Time Interval	Duration
Early Morning	0:00 - 1:00
Day Time Interval 1	7:00 - 9:00
Day Time Interval 2	17:00 - 19:00
Late Night	22:00 - 23:00

Table 5: Parameter settings of our model.

Parameters	Values
Memory buffer size	10000
Model update step	1 episode
Target update step C	2 episodes
$C1$	3000
γ	0.99
ϵ	$1 \rightarrow 0.05$ (linear decay)
Relation reasoning step d	2
batch size	64

- **Grid_{3×3}**: A 3×3 grid network. The origins and destinations of vehicles in this road network are set to any edges uniformly at random. The vehicle arrival rate is 1.8 which is stable for simulation and indicates that 1.8 vehicles are generated per second in the road network.
- **Grid_{6×6}**: A large-scale 6 × 6 grid network, in which two kinds of traffic patterns are generated, i.e., *Unidirect_{6×6}* and *Bidirect_{6×6}* for unidirectional and bidirectional traffic pattern respectively. The traffic comes uniformly with 600 vehicles/lane/hour in West-East direction and 180 vehicles/lane/hour in South-North direction.

For synthetic data, we used four phases to control the traffic movements for the intersection, i.e., WE-Straight (Going Straight from both West and East), WE-Left (Turning Left from both West and East), SN-Straight (Going Straight from both South and North), SN-Left (Turning Left from both South and North).

5.1.2 Real-world Dataset. The real-world dataset was collected in a medium-sized city from China. Totally, in this dataset, there are four traffic lights as shown in Figure 1 (a), which contain the

information of vehicles and roads recorded by the camera in the nearby intersection facing to the vehicles, as well as corresponding timestamps over the time period from 11/06/2018 to 11/12/2018. After analyzing these records, the trajectory for each vehicle could be captured. As shown in Table 2, the traffic arrival rate, i.e., the average amount of arriving vehicles during one second, is significantly variant in a different time.

For the real-world dataset, We adopt the traffic phases currently applied in the real world as shown in Table 3. It can be seen that there are different kinds of traffic phases for different intersections at different times. More detailed traffic phase configurations are attached to the appendix in the supplementary material. According to the Table 3, we can find that there exist three periods, namely the early morning (0:00 - 6:00), day time (6:30 - 20:30) and late night (20:30 - 24:00). During each period, most traffic lights, e.g., light 1, 3 and 4 will execute different phase plans. Thus, to validate the effectiveness, we separately selected four-time frames from these three periods, as shown in Table 4 as one episode. For fully reflecting the traffic status during day time, we selected two frames, which correspond to the morning/evening peaks respectively. Further analysis of time division will be introduced in Section 5.2.3.

To simulate the traffic status under different settings of traffic lights, we then utilized a widely-used traffic simulator, called Simulation of Urban MObility (SUMO) ¹. Both synthetic and real datasets are fed into SUMO for simulation.

5.1.3 Evaluation Metric. Following the previous researches [24, 38], we adopt the commonly used **average travel time** metric to evaluate the performance of different methods. This metric is defined as the average travel time for all the vehicles traveling from their origins to destinations, which people care the most in practice.

5.1.4 Implementation Details. The parameters for our model are summarized in Table 5. Particularly, each action of agent will last for 10 seconds, which was searched among {5, 10, 15}. To stabilize the training process, we pre-trained the model using fixed time control strategy by setting all the traffic light phase to a fixed time p_t , where p_t was selected in {15, 20, 25, 30, 35, 40, 45} and trained for 40,000 steps. Besides, the temporal dependency interval Δt was searched among {20, 30, 60, 90, 120}, the ϵ for ϵ -greedy policy was linearly decayed for the first 10 episodes, and the hidden size for both edge encoder and output layer were set to 64. Finally, all the parameters were initialized using He initialization in [15], and then trained using Adam [19] algorithm with learning rate as 0.001 and gradient clipping value as 10.

5.1.5 Compared Methods. To validate the effectiveness of STMARL framework, several state-of-the-art methods are selected as baseline methods, which are listed as follows:

- **Fixed-time Control: (Fixed-time)** [25], which uses a pre-defined plan for traffic light control. For the real-world dataset, we directly adopt the phase plan in the real world. More details are in the supplementary material.
- **Self-Organizing Traffic Light Control (SOTL)** [9], which is an actuated traffic light control method. Here the decisions to change traffic light phase are based on the current traffic

state, including eclipsed time and the number of vehicles approaching the red light.

- **Max-Plus Coordination for Urban Traffic Control (Max-Plus)** [21], which uses max-plus [20] algorithm for modeling the coordination among agents. For a fair comparison, Max-Plus shares the same state, action, and reward definition with STMARL.

Besides, the following variations of our method are compared:

- **Base**, which is the independent DQN method with shared parameters among the agents.
- **Base+Graph**, which incorporates the spatial structure information for iterative relational reasoning.
- **Base+Graph+Time**, which is our full model (STMARL) not only considering the spatial structure dependency, but also incorporating the historical traffic information.

All the methods are turned to report the best performance. For the reinforcement learning methods, we trained the model for 80 episodes and test for 20 episodes with epsilon $\epsilon = 0.05$.

5.2 Experimental Results

5.2.1 Overall Result. In this section, we compared the proposed method with the baseline methods on both synthetic and real-world datasets. The performance is shown in Table 6. We can observe that our proposed STMARL method significantly outperforms all the baseline methods in all datasets.

For the comparison of performance across different datasets, we observed that the performance gap becomes significantly larger with the increasing scale of road network. For example, STMARL outperforms the best baseline by 13.2% in dataset *Unidirec_{6x6}*. There also exists a significant margin between STMARL model and baseline methods under different traffic patterns, i.e., uniformly at random, unidirectional, bidirectional and real-world dynamic traffic.

Compared with baseline methods, we observed that STMARL outperforms the traditional traffic light control methods (Fixed-time and SOTL) with a significant margin. This phenomenon demonstrates the effectiveness of the reinforcement learning methods which change traffic phases adaptively to optimize the long term traffic situation.

Besides, our STMARL model significantly outperforms the Max-Plus baseline which also considers the coordination among traffic lights, demonstrating the efficient coordination strategy by learning spatial-temporal dependency in our model. Moreover, our model is more stable with a lower standard deviation.

For the model variants, learning spatial structure dependency (Base+Graph) significantly outperforms the Base model. The reason is that the Base model ignores the spatial structure information among the traffic lights. Incorporating the historical traffic state information (Base+Graph+Time) further improves performance. Figure 4 illustrates the training curves of these model variants across different datasets. It can be observed that (Base+Graph) model constantly outperforms the Base model by a significant margin in all datasets. Moreover, (Base+Graph+Time) outperforms (Base+Graph) significantly with faster convergence speed. These quantitative results clearly demonstrate the effectiveness of jointly learning

¹<http://sumo.dlr.de/index.html>

Table 6: Performance comparison on the synthetic data and real-world data w.r.t. average travel time (in seconds, the lower the better). The number is mean value \pm standard deviation. * indicates the improvement of STMARL over the best baseline is significant based on paired t-test at the significance level of $p < 0.01$.**

Methods	$Grid_{3 \times 3}$	$Unidirec_{6 \times 6}$	$Bidirect_{6 \times 6}$	$D_{realworld}$
Fixed-time	241.361 \pm 19.042	746.134 \pm 7.33	746.413 \pm 6.761	116.584 \pm 5.185
SOTL	493.074 \pm 4.414	425.712 \pm 31.248	540.270 \pm 43.355	142.663 \pm 7.892
Max-Plus	440.994 \pm 20.539	751.803 \pm 131.003	637.515 \pm 9.833	75.356 \pm 5.489
Base	285.797 \pm 13.744	337.175 \pm 5.587	307.141 \pm 2.822	77.926 \pm 6.515
Base+Graph	171.896 \pm 2.494	326.491 \pm 7.749	296.553 \pm 2.206	74.840 \pm 5.217
Base+Graph+Time(STMARL)	163.325* \pm 9.19	283.478* \pm 2.619	272.589* \pm 2.599	73.528* \pm 5.399

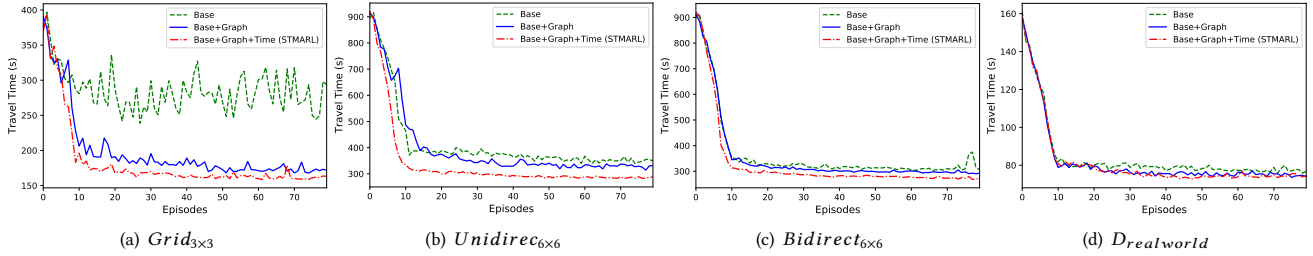


Figure 4: Training curve of our model variants across different datasets.

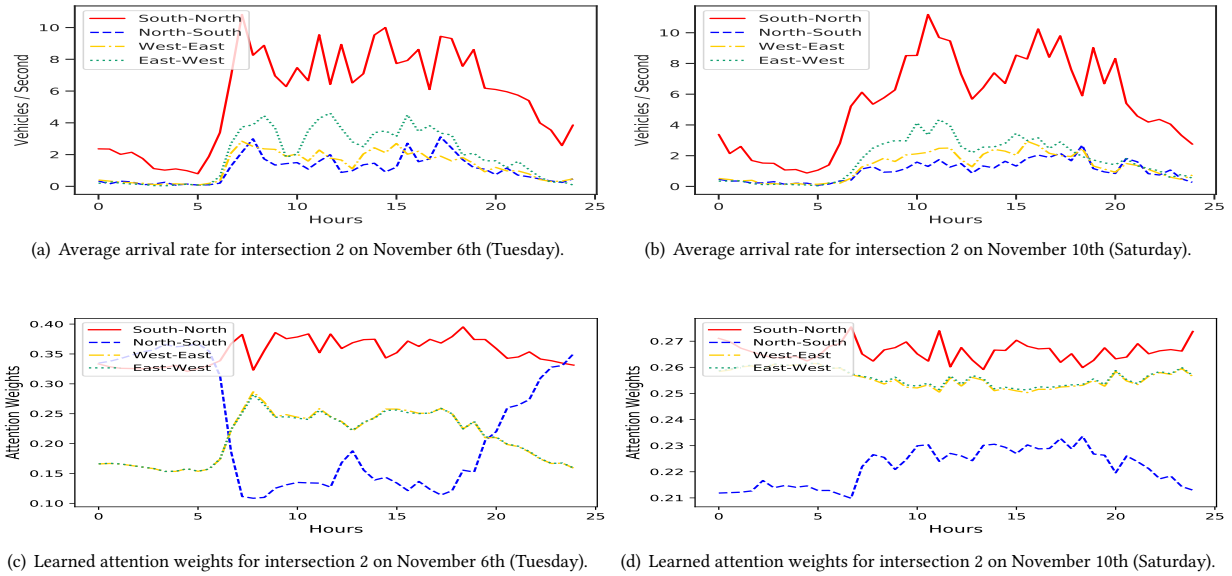


Figure 5: Average arriving vehicles ((a), (b)) and learned attention weights ((c), (d)) by STMARL model on the four incoming edges (e.g., South-North means the edge direction is from South to North connected to this intersection) of intersection 2 (node TL 2 in Figure 1) On November 6th (Tuesday) and November 10th (Saturday), 2018.

spatial structure information and temporal dependency for multi-intersection traffic light control.

5.2.2 *Sensitiveness of Temporal Dependency Interval Δt .* Figure 6 shows the performance of STMARL model with different temporal

dependency interval Δt . We found that STMARL achieves the best performance when $\Delta t = 60s, 90s, 60s, 30s$ for $Grid_{3 \times 3}, Unidirec_{6 \times 6}, Bidirect_{6 \times 6}$ and $D_{realworld}$ respectively. These results indicate that a relatively medium time interval Δt should be more appropriate to learn the temporal dependency.

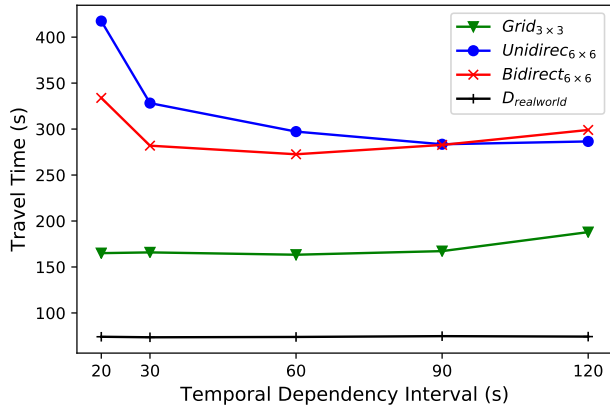


Figure 6: Performance of STMARL model with different temporal dependency interval Δt across all the datasets.

Table 7: Learned phase duration of STMARL model.

Traffic Light ID	Time Interval	Phase ID	Phase Duration (Seconds)	
			Average Phase Duration learned by STMARL	Fixed Time Phase Duration
Traffic Light 1	Early Morning	12, 13, 14, 15, 16	12, 11, 27, 11, 11	35, 25, 40, 11, 34
	Day Time Interval 1	12, 13, 14, 15, 16	18, 20, 54, 11, 12	40, 30, 41, 16, 35
	Day Time Interval 2	12, 13, 14, 15, 16	21, 15, 50, 11, 12	40, 30, 41, 16, 35
	Late Night	12, 13, 14, 15, 16	12, 11, 39, 11, 11	35, 25, 40, 11, 34
Traffic Light 3	Early Morning	4, 5	25, 14	15, 15
	Day Time Interval 1	6, 7, 5	19, 12, 11	42, 25, 17
	Day Time Interval 2	6, 7, 5	22, 11, 11	42, 25, 17
	Late Night	4, 5	23, 12	35, 15

5.2.3 *Qualitative Study.* In this section we provide further analysis of the learned traffic phase duration, attention weights to the adjacent nodes and emergence of the green wave learned by the STMARL model in the real-world dataset.

Analysis of the Traffic Phase Duration. Table 7 shows the learned average phase duration by our model over the selected time interval (Table 4). Taking Traffic Light 1 as an example, we observe that the learned phase duration for early morning and late night is quite different especially for phase 14, while current applied fixed time plan uses the same duration for both time periods. For the day time in interval 1 and interval 2, the learned phase duration is also quite different, while the fixed time plans currently used are still the same.

However, the opposite time changing can be observed for Traffic Light 3. Therefore, currently used divided time interval in the real world can be further improved by merging the time interval with a similar phase duration, while those intervals with different phase duration should be split.

Interpretation of Attention Weights. In this section, we analyze the learned attention weights for the traffic light agent and take the Traffic Light agent 2 as an example. Figure 5 (c)(d) shows the learned attention weights in four incoming edges from its neighbors on Tuesday and Saturday. We also show the average number of approaching vehicles in corresponding edges in Figure 5 (a)(b). It can be observed that the learned attention weights keep pace with the dynamic number of vehicles in the corresponding edges. For example, in different peak hour, the attention weights in the corresponding edge directions also become larger.

Moreover, in Figure 5(c), the attention weight of the South-North direction is the largest compared to the other three directions in most cases, which corresponds to the largest arriving vehicle numbers as shown in Figure 5(a). Similar rule could be found between Figure 5(d) and Figure 5(b). Therefore, the larger attention weights make the Traffic Light agent 2 care more about the downstream traffic situation which may spill into intersection 2. As a result, the Traffic Light agent 2 was influenced by the decision of Traffic Light agent 1. Along this line, the coordination among Traffic Light agent 2 and agent 1 is crucial so as not to cause severe traffic congestion to Intersection 2 due to the large traffic flow from intersection 1. Therefore, the larger attention weights in the edge direction may indicate that it's more necessary to coordinate among these two agents.

Coordination for Green Wave. The green wave occurs when a series of traffic lights are coordinated to allow continuous traffic flow over several intersections along one main direction. Therefore, it can be used to test the coordination mechanism learned by multiple traffic lights. Figure 7 shows the dynamics of traffic light phase learned by our model (Figure 7 (a)(b)(c)) and the corresponding number of approaching cars along North-South direction (Figure 7 (d)(e)(f)) which shows the emergence of *green wave* phenomenon. It can be observed that from Figure 7 (a)(b)(c), in these three time periods, there exists green wave, i.e., green arrow, where all the four traffic light agents coordinated their traffic phases to allow fast traveling for the approaching cars. Figure 7 (d)(e)(f) shows that the green wave significantly accelerates the traffic flow by reducing the maximum number of vehicles approaching one intersection (e.g., the intersection controlled by Traffic Light 1). Therefore, the green wave demonstrates that STMARL model can learn coordination policy to reduce the traffic congestion in the integral level.

6 CONCLUSIONS

In this paper, we proposed the Spatio-Temporal Multi-Agent Reinforcement Learning (STMARL) model for multi-intersection traffic light control. The proposed STMARL model can leverage the spatial structure in the real world to facilitate coordination among multiple traffic lights. Moreover, it also considers the historical traffic information for current decision making. Specifically, we first construct the traffic light adjacency graph based on the spatial structure among traffic lights. Then, historical traffic records will be integrated with current traffic status via Recurrent Neural Network structure. Moreover, based on the temporally-dependent traffic information, we design a Graph Neural Network based model to represent relationships among multiple traffic lights, and the decision for each traffic light will be made in a distributed way by deep Q-learning method. Experiments on both synthetic and real-world datasets have demonstrated the effectiveness of our STMARL framework, which also provides an insightful understanding of the influence mechanism among multi-intersection traffic lights.

REFERENCES

- [1] Baher Abdulhai, Rob Pringle, and Grigoris J Karakoulas. 2003. Reinforcement learning for true adaptive traffic signal control. *Journal of Transportation Engineering* 129, 3 (2003), 278–285.
- [2] Itamar Arel, Cong Liu, T Urbanik, and AG Kohls. 2010. Reinforcement learning-based multi-agent system for network traffic signal control. *IET Intelligent Transport Systems* 4, 2 (2010), 128–135.

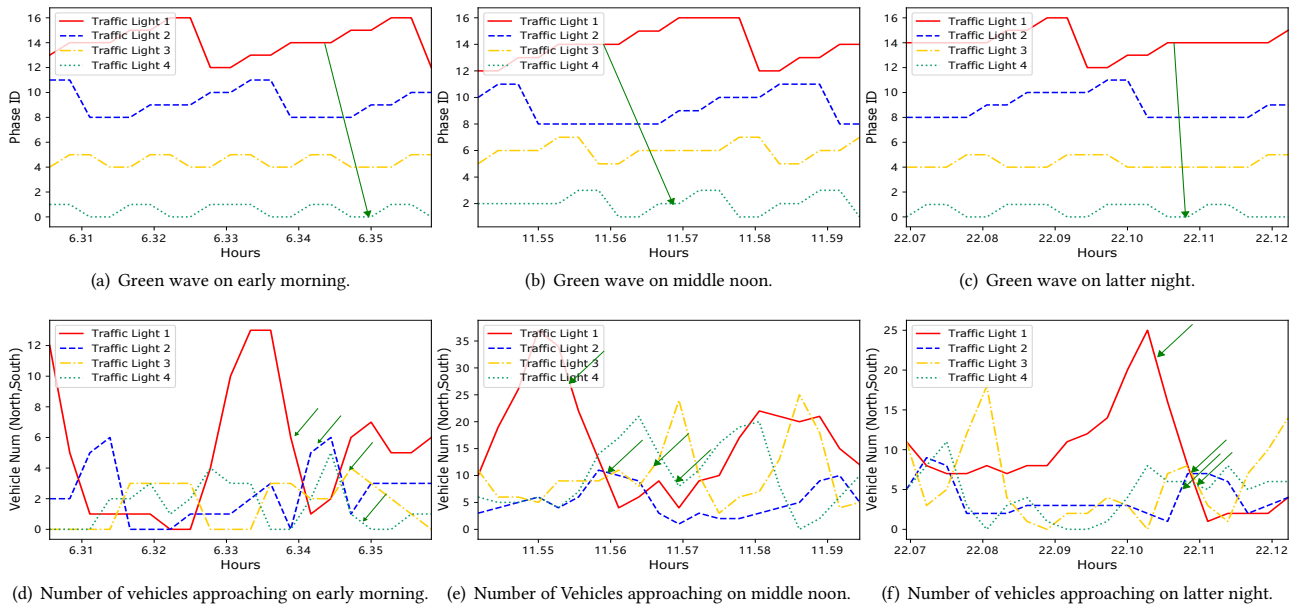


Figure 7: The emerging green waves show in different time periods on November 6th, 2018, in which the waves pointed by the green arrows indicate the green phases of traffic lights in North-South direction.

[3] Peter Battaglia, Razvan Pascanu, Matthew Lai, Danilo Jimenez Rezende, et al. 2016. Interaction networks for learning about objects, relations and physics. In *Advances in neural information processing systems*. 4502–4510.

[4] Peter W Battaglia, Jessica B Hamrick, Victor Bapst, Alvaro Sanchez-Gonzalez, Vinicius Zambaldi, Mateusz Malinowski, Andrea Tacchetti, David Raposo, Adam Santoro, Ryan Faulkner, et al. 2018. Relational inductive biases, deep learning, and graph networks. *arXiv preprint arXiv:1806.01261* (2018).

[5] Tim Brys, Tong T Pham, and Matthew E Taylor. 2014. Distributed learning and multi-objectivity in traffic light control. *Connection Science* 26, 1 (2014), 65–83.

[6] Lucian Buesoni, Robert Babuska, and Bart De Schutter. 2008. A comprehensive survey of multiagent reinforcement learning. *IEEE Transactions on Systems, Man, And Cybernetics-Part C: Applications and Reviews*, 38 (2), 2008 (2008).

[7] CityLab. 2018. Traffic’s Mind-Boggling Economic Toll. (2018). <https://www.citylab.com/transportation/2018/02/traffics-mind-boggling-economic-toll/552488/>

[8] Djork-Arné Clevert, Thomas Unterthiner, and Sepp Hochreiter. 2015. Fast and accurate deep network learning by exponential linear units (elus). *arXiv preprint arXiv:1511.07289* (2015).

[9] Seung-Bae Cools, Carlos Gershenson, and Bart D’Hooghe. 2013. Self-organizing traffic lights: A realistic simulation. In *Advances in applied self-organizing systems*. Springer, 45–55.

[10] Samah El-Tantawy and Baher Abdulhai. 2010. An agent-based learning towards decentralized and coordinated traffic signal control. In *13th International IEEE Conference on Intelligent Transportation Systems*. IEEE, 665–670.

[11] Samah El-Tantawy, Baher Abdulhai, and Hossam Abdelgawad. 2013. Multiagent reinforcement learning for integrated network of adaptive traffic signal controllers (MARLIN-ATSC): methodology and large-scale application on downtown Toronto. *IEEE Transactions on Intelligent Transportation Systems* 14, 3 (2013), 1140–1150.

[12] Jakob Foerster, Ioannis Alexandros Assael, Nando de Freitas, and Shimon Whiteson. 2016. Learning to communicate with deep multi-agent reinforcement learning. In *Advances in Neural Information Processing Systems*. 2137–2145.

[13] Justin Gilmer, Samuel S. Schoenholz, Patrick F. Riley, Oriol Vinyals, and George E. Dahl. 2017. Neural Message Passing for Quantum Chemistry. In *Proceedings of the 34th International Conference on Machine Learning, ICML*. 1263–1272.

[14] Jayesh K Gupta, Maxim Egorov, and Mykel Kochenderfer. 2017. Cooperative multi-agent control using deep reinforcement learning. In *International Conference on Autonomous Agents and Multiagent Systems*. Springer, 66–83.

[15] Kaiming He, Xiangyu Zhang, Shaoqing Ren, and Jian Sun. 2015. Delving deep into rectifiers: Surpassing human-level performance on imagenet classification. In *Proceedings of the IEEE international conference on computer vision*. 1026–1034.

[16] Sepp Hochreiter and Jürgen Schmidhuber. 1997. Long short-term memory. *Neural computation* 9, 8 (1997), 1735–1780.

[17] Jiechun Jiang, Chen Dun, and Zongqing Lu. 2018. Graph Convolutional Reinforcement Learning for Multi-Agent Cooperation. *arXiv preprint arXiv:1810.09202* (2018).

[18] Mohamed A Khamis and Walid Gomaa. 2014. Adaptive multi-objective reinforcement learning with hybrid exploration for traffic signal control based on cooperative multi-agent framework. *Engineering Applications of Artificial Intelligence* 29 (2014), 134–151.

[19] Diederik P Kingma and Jimmy Ba. 2014. Adam: A method for stochastic optimization. *arXiv preprint arXiv:1412.6980* (2014).

[20] Jelle R Kok and Nikos Vlassis. 2006. Collaborative multiagent reinforcement learning by payoff propagation. *Journal of Machine Learning Research* 7, Sep (2006), 1789–1828.

[21] Lior Kuyper, Shimon Whiteson, Bram Bakker, and Nikos Vlassis. 2008. Multiagent reinforcement learning for urban traffic control using coordination graphs. In *Joint European Conference on Machine Learning and Knowledge Discovery in Databases*. Springer, 656–671.

[22] Yujia Li, Daniel Tarlow, Marc Brockschmidt, and Richard Zemel. 2015. Gated graph sequence neural networks. *arXiv preprint arXiv:1511.05493* (2015).

[23] Ryan Lowe, Yi Wu, Aviv Tamar, Jean Harb, OpenAI Pieter Abbeel, and Igor Mordatch. 2017. Multi-agent actor-critic for mixed cooperative-competitive environments. In *Advances in Neural Information Processing Systems*. 6379–6390.

[24] Patrick Mannion, Jim Duggan, and Enda Howley. 2016. An experimental review of reinforcement learning algorithms for adaptive traffic signal control. In *Autonomous Road Transport Support Systems*. Springer, 47–66.

[25] Alan J Miller. 1963. Settings for fixed-cycle traffic signals. *Journal of the Operational Research Society* 14, 4 (1963), 373–386.

[26] Volodymyr Mnih, Koray Kavukcuoglu, David Silver, Andrei A Rusu, Joel Veness, Marc G Bellemare, Alex Graves, Martin Riedmiller, Andreas K Fidjeland, Georg Ostrovski, et al. 2015. Human-level control through deep reinforcement learning. *Nature* 518, 7540 (2015), 529.

[27] Ranjit Nair, Pradeep Varakantham, Milind Tambe, and Makoto Yokoo. 2005. Networked distributed POMDPs: A synthesis of distributed constraint optimization and POMDPs. In *AAAI*, Vol. 5. 133–139.

[28] Norihiko Ono and Kenji Fukumoto. 1996. Multi-agent reinforcement learning: A modular approach. In *Second International Conference on Multiagent Systems*. 252–258.

[29] Liviu Panait and Sean Luke. 2005. Cooperative multi-agent learning: The state of the art. *Autonomous agents and multi-agent systems* 11, 3 (2005), 387–434.

[30] Franco Scarselli, Marco Gori, Ah Chung Tsoi, Markus Hagenbuchner, and Gabriele Monfardini. 2009. The graph neural network model. *IEEE Transactions on Neural Networks* 20, 1 (2009), 61–80.

- [31] Merlijn Steingrover, Roelant Schouten, Stefan Peelen, Emil Nijhuis, Bram Bakker, et al. 2005. Reinforcement Learning of Traffic Light Controllers Adapting to Traffic Congestion. In *BNAIC*. Citeseer, 216–223.
- [32] Sainbayar Sukhbaatar, Rob Fergus, et al. 2016. Learning multiagent communication with backpropagation. In *Advances in Neural Information Processing Systems*. 2244–2252.
- [33] Ardi Tampuu, Tambet Matiisen, Dorian Kodelja, Ilya Kuzovkin, Kristjan Korjus, Juhan Aru, Jaan Aru, and Raul Vicente. 2017. Multiagent cooperation and competition with deep reinforcement learning. *PloS one* 12, 4 (2017), e0172395.
- [34] Ming Tan. 1993. Multi-agent reinforcement learning: Independent vs. cooperative agents. In *Proceedings of the tenth international conference on machine learning*. 330–337.
- [35] Ashish Vaswani, Noam Shazeer, Niki Parmar, Jakob Uszkoreit, Llion Jones, Aidan N Gomez, Lukasz Kaiser, and Illia Polosukhin. 2017. Attention is all you need. In *Advances in Neural Information Processing Systems*. 5998–6008.
- [36] Petar Velickovic, Guillem Cucurull, Arantxa Casanova, Adriana Romero, Pietro Lio, and Yoshua Bengio. 2017. Graph attention networks. *arXiv preprint arXiv:1710.10903* 1, 2 (2017).
- [37] Tingwu Wang, Renjie Liao, Jimmy Ba, and Sanja Fidler. 2018. Nervenet: Learning structured policy with graph neural networks. (2018).
- [38] Hua Wei, Guanjie Zheng, Huaxiu Yao, and Zhenhui Li. 2018. Intellilight: A reinforcement learning approach for intelligent traffic light control. In *Proceedings of the 24th ACM SIGKDD International Conference on Knowledge Discovery & Data Mining*. ACM, 2496–2505.
- [39] Kok-Lim Alvin Yau, Junaid Qadir, Hooi Ling Khoo, Mee Hong Ling, and Peter Komisarczuk. 2017. A survey on reinforcement learning models and algorithms for traffic signal control. *ACM Computing Surveys (CSUR)* 50, 3 (2017), 34.
- [40] Biao Yin, Mahjoub Dridi, and Abdellah El Moudni. 2016. Traffic network micro-simulation model and control algorithm based on approximate dynamic programming. *IET Intelligent Transport Systems* 10, 3 (2016), 186–196.
- [41] Vinicius Zambaldi, David Raposo, Adam Santoro, Victor Bapst, Yujia Li, Igor Babuschkin, Karl Tuyls, David Reichert, Timothy Lillicrap, Edward Lockhart, et al. 2018. Relational Deep Reinforcement Learning. *arXiv preprint arXiv:1806.01830* (2018).
- [42] Erik Zawadzki, Asher Lipson, and Kevin Leyton-Brown. 2014. Empirically evaluating multiagent learning algorithms. *arXiv preprint arXiv:1401.8074* (2014).

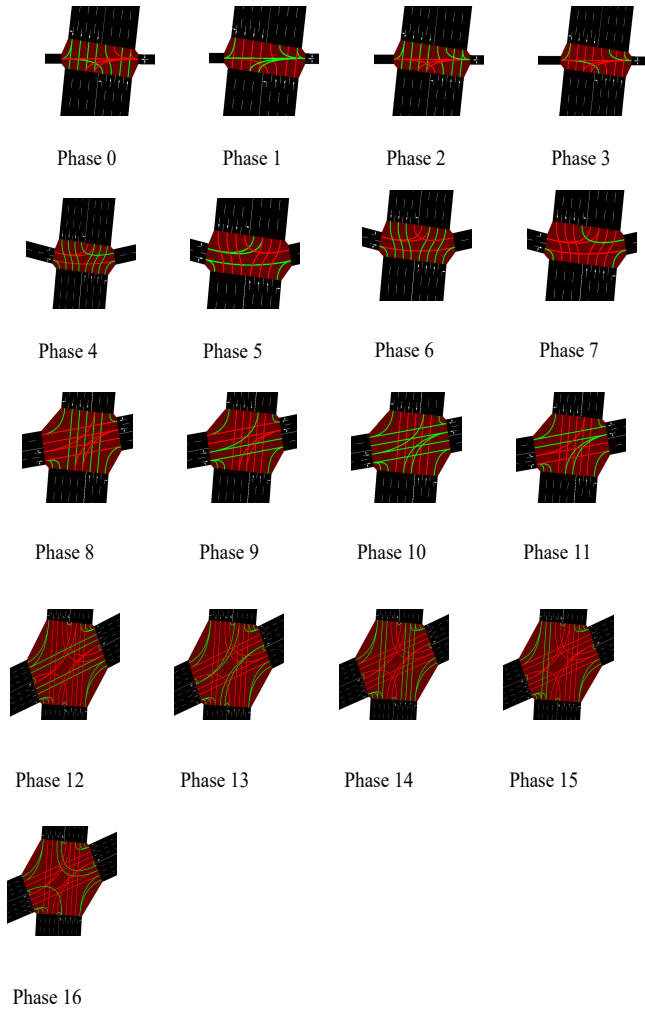


Figure 8: Detailed phase configuration for the traffic lights used in the real-world dataset.

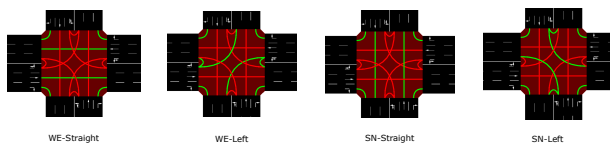


Figure 9: Phase configuration (in order) for the traffic lights used in the synthetic datasets.

A APPENDIX

Table 8: Fixed-time plan in the real-world.

Traffic Light ID	Time Range	Phase ID (In Order)	Duration (Seconds)
Traffic Light 1	0:00-6:00	12, 13, 14, 15, 16	35, 25, 40, 11, 34
	6:00-20:30	12, 13, 14, 15, 16	40, 30, 41, 16, 35
	20:30-24:00	12, 13, 14, 15, 16	35, 25, 40, 11, 34
Traffic Light 2	0:00-24:00	8, 9, 10, 11	48, 11, 13, 15
Traffic Light 3	0:00-6:30	4, 5	15, 15
	6:30-20:30	6, 7, 5	42, 25, 17
	20:30-24:00	4, 5	35, 15
Traffic Light 4	0:00-6:30	0, 1	15, 15
	6:30-20:30	2, 3, 1	43, 15, 29
	20:30-24:00	0, 1	25, 15

A.1 Traffic Light Phase Configuration

A.1.1 *Traffic Light Phases for Synthetic Data.* Figure 9 shows Traffic light phases used in the synthetic datasets. The change of each phase is followed by the 3 seconds yellow light.

A.1.2 *Traffic Light Phases for Real-world Data.* We provide all the phases configuration used by the four traffic lights for the real-world dataset in Figure 8. The change of each phase is followed by the 3 seconds yellow light except Phase 9. Each traffic light’s phase id list is shown in Table 3 in the main text.

A.2 Fixed-time Plan

Phase duration of fixed-time plan used in the real-world is listed in Table 8.

A.3 Simulation Setting

For the synthetic data, each intersection has four directions and each road segment has 3 lanes (300 meters long and 3.2 meters width). The road network in the real data is imported from OpenStreetMap².

²<https://www.openstreetmap.org>